ELECTROHYDRODYNAMIC DISPERSION OF DEFORMABLE AEROSOLS IN THE PRESENCE OF AN ELECTRIC FIELD AND CHEMICAL REACTION USING TAYLOR DISPERSION MODEL*

RUDRAIAH N, DEVARAJU N
UGC-CAS in Fluid Mechanics, Department of Mathematics, Bangalore University, Bangalore – 560 001, India
National Research Institute for Applied Mathematics (NRIAM), #462/G, 7th Cross, 7th Block (West) Jayanagar, Bangalore – 560 070, India

NG Chiu-On
Department of Mechanical Engineering, The University of Hong Kong, Pokfulam Road, Hong Kong, China

ABSTRACT Under the effects of electric field and chemical reaction, the problem of dispersion of aerosols in a poorly conducting fluid in a channel is solved analytically using the mixture theory together with a regular perturbation technique. It is shown that the aerosols are dispersed relative to a plane moving with the mean speed of atmospheric fluid as well as the mean speed of agglomeration of aerosol with a relative diffusion coefficient, called Taylor dispersion coefficient. This coefficient is numerically computed and the results reveal that it increases with an increase in the Electric number, but decreases with an increasing porous parameter. The physical explanations for the same are given in this paper.

Keywords: dispersion, aerosols, electrohydrodynamics, mixture theory

1. Introduction

This paper deals with the effects of electric field and chemical reaction on the dispersion of deformable aerosols in a poorly conducting atmospheric fluid flowing in a channel bounded by porous layers using Taylor's [1] model.

Electric fields are used extensively in different industrial problems particularly in those concerned with chemical, electrical, electronic and drug industries for various separation processes. Waterman [2] had reviewed the process of using electric fields

to improve coalescence and found these techniques to be quite effective in the removal of water from oil. Williams and Bailey [3] examined coalescence of poorly conducting drops in the presence of an electrical field both theoretically and experimentally. Schmidt [4] performed experiments with different aerosols and observed that the application of an electric field had the effect of reducing sedimentation time. A detailed calculation of the aerosol particles and size distribution suggests that this phenomenon of reduction of sedimentation time is due to the electric field enhancing aerosol particle coalescence.

Studies to predict the collision frequencies of settling mechanisms have been carried out in the past. Also, the deposition of nano-particles under different conditions was investigated in the recent numerical studies by Sun *et al.* [5], Gan *et al.* [6], Yin and Lin [7], and Liu and Lin [8]. Wang *et al.* [9] used a trajectory analysis for estimating the aggregation rates and found that the electric fields can enhance the gravitational settling of charged particles.

Usually, when the Earth's local weather is fair, the electric field is about 180-280 Vm^{-1} depending on the concentration of aerosols (see Jayaratne and Verma [10]). When the aerosols are in continuous deformation with relative motion resulting in particles colliding and coalescing to form larger particles where an electric field induces a dipole in uncharged aerosol particles, as explained by Rudraiah and Devaraju [11], who showed that the charges induced on the closest sides of the neighboring particles are of opposite sign. These particles experience an attractive force which can eventually lead to the particles colliding causing agglomeration or coalescence. That is, the difference in number concentration of aerosols causes variation in electrical conductivity σ, which releases the charges forming distribution of charge density ρ_{ε}. These charges produce an induced electric field, $\vec{E}_{ind}$, known as concentration electric field. In addition, there may be an applied electric field, $\vec{E}_a$, due to embedded electrodes of different potentials at the boundaries. The total electric field $\vec{E}_t = \vec{E}_{ind} + \vec{E}_a$ produces not only a current density, $\vec{J}$, according to Ohm's law, but also an electric force $\rho_e \vec{E}_t$, which is computed using Maxwell's equations.

The motion of atmospheric fluid is usually turbulent due to large length scales which result in large Reynolds number. Therefore, to derive the required basic equations, we use the mechanism of mixture of aerosols and atmospheric turbulent fluid taking into account the combined effect of electric field, deformable aerosols and settling of large particles on primary as well as secondary admixture using Reynolds Averaging Procedure supplemented with gradient diffusion model. The primary pollutants, directly injected into the atmosphere, are assumed to satisfy the general equation involving the relative velocity between aerosol and atmospheric fluid. The aerosol medium is assumed to be homogeneous, incompressible and isotropic in the presence of the body force. In the literature (Kenyon [12], Bowen [13] and Barry *et al.* [14], Rudraiah and Devaraju [11]) mixture theory has been used to derive the basic equations for an ordinary fluid in the absence of electric field assuming the mixture of aerosol and atmospheric fluid as deformable porous media. The dispersion of aerosols and other suspended particulate matter (SPM) in the presence of electric field in atmospheric turbulent fluid has not been given much attention in the literature. The study of it is the main objective of this paper because of its importance in many applications discussed above. To achieve the objectives of this paper, the required basic equations, relevant boundary conditions and the dimensionless form are given in section 2 on mathematical formulation of this paper.

Analytical solutions of coupled partial differential equations are derived in section 3 of this paper using regular perturbation technique with a perturbation parameter ε. The Taylor dispersion coefficient for atmospheric fluid and also for aerosols are determined in this section. These dispersion coefficients, the velocity for atmospheric fluid u^f and for aerosols u^s are numerically computed and the results are represented graphically and important conclusions are given in section 4.

2. Mathematical formulation

We consider a two-dimensional geometry as shown in Figure 1. It consists of flow through a symmetrical channel extended to infinity on both directions of *x*-axis. The channel is filled with poorly conducting fluid saturated porous media regarded as a mixture of aerosol and atmospheric fluid bounded by permeable layers with embedded electrodes of different potentials at $y = 0$ and $y = h$. The applied

pressure gradient $\partial p / \partial x = G(t)$ produces an axially directed flow. For an infinite channel, we assume fully developed unidirectional flow as in Taylor [1] so that there is no x-dependence in any of the physical quantities except the pressure, electric potential and concentration of aerosols. The unidirectional flow is represented with velocities $q_1^s = u^s$ as the x-component of aerosol and $q_1^f = u^f$ the x-component of atmospheric fluid. Then the required momentum equations are given by

$$\overline{\rho^\beta}\left[\frac{\partial \overline{q_i^\beta}}{\partial t} + \overline{q_j^\beta}\frac{\partial \overline{q_i^\beta}}{\partial x_j}\right] = -\phi^\beta \frac{\overline{\partial p}}{\partial x_i} + \left[X_p\left(\mu - \mu_a\right) + \mu_a + \mu_e\right]\frac{\partial^2 \overline{q_i^\beta}}{\partial x_j \partial x_j} \mp K\left(\overline{q_i^s} - \overline{q_i^f}\right) + \rho_e E_t. \tag{1}$$

These equations, following Rudraiah and Devaraju [11], for the mixture of aerosol and atmospheric turbulent fluid with the assumptions stated above becomes,

$$\rho^s \frac{\partial u^s}{\partial t} = \mu_s \frac{\partial^2 u^s}{\partial y^2} - \phi^s G - K\left(u^s - u^f\right) + \rho_e E_x, \tag{2}$$

$$\rho^f \frac{\partial u^f}{\partial t} = \mu_f \frac{\partial^2 u^f}{\partial y^2} - \phi^f G + K\left(u^s - u^f\right) + \rho_e E_x, \tag{3}$$

where the superscript, s, represents solid phase (i.e. aerosol) and, f, the fluid phase (i.e. atmospheric poorly conducting fluid), $\mu_s = \mu + \mu_e$ is one of the turbulent Lame constants, $\mu_f = \mu_a + \mu_e$ the effective viscosity (also called Brinkman viscosity) of poorly conducting atmospheric turbulent fluid, μ the Lamé constant, μ_e the eddy viscosity, K the linear drag coefficient that is Darcy resistance offered by solid to fluid, G the pressure gradient, φ^s the aerosol volume fraction and φ^f is the fluid volume fraction. We make these equations dimensionless using

$$\eta = \frac{y}{h}, \quad t^* = \frac{t}{t_0}, \quad u^{s*} = \frac{\mu_s}{h^2 G_0}u^s, \quad u^{f*} = \frac{\mu_f}{h^2 G_0}u^f, \quad G^* = \frac{G}{G_0},$$
$$E_x^* = \frac{E_x}{V/h}, \quad \rho_e^* = \frac{\rho_e}{\varepsilon_0 V/h^2}, \quad \Phi^* = \frac{\Phi}{V}, \quad v^f = \frac{\mu_f}{\rho^f}, \quad v^s = \frac{\mu_s}{\rho^s} \tag{4}$$

where h, G_0, V and t_0 are the characteristic length, pressure gradient, electric potential and time respectively and the asterisks (*) denote the dimensionless quantities.

Substituting Eq. (4) into Eqs. (2) and (3), simplifying and for simplicity neglecting the asterisks, we get

$$\frac{\partial u^s}{\partial t} = R_1 \frac{\partial^2 u^s}{\partial \eta^2} - R_1 \phi^s G - R_2 \left(u^s - R_3 u^f \right) + W_e \rho_e E_x, \tag{5}$$

$$\frac{\partial u^f}{\partial t} = R_4 \frac{\partial^2 u^f}{\partial \eta^2} - R_4 \phi^s G + R_2 \lambda \left(u^s - R_3 u^f \right) + W_e \rho_e E_x, \tag{6}$$

where R_i $(i = 1$ to $4)$ are dimensionless parameters defined by

$$R_1 = \frac{\mu_s t_0}{\rho^s h^2}, \quad R_2 = \frac{K t_0}{\rho^s}, \quad R_3 = \frac{\mu_s}{\mu_f}, \quad R_4 = \frac{\mu_f t_0}{\rho^f h^2}, \quad \lambda = \frac{v^f}{v^s},$$

$$W_e = \frac{\varepsilon_0 V^2}{\rho^s h^2 (\bar{u}^s)^2} = \frac{\varepsilon_0 V^2}{\rho^f h^2 (\bar{u}^f)^2} \tag{7}$$

The boundary conditions are the Saffman [15] slip conditions of the form

$$\frac{du^s}{d\eta} = \pm \alpha_1 \sigma_p u^s, \quad \frac{du^f}{d\eta} = \pm \alpha_2 \sigma_p u^f, \text{ at } \eta = 0 \text{ and } 1 \text{ for } t > 0, \text{ respectively} \tag{8}$$

where $\sigma_p = h/\sqrt{k}$ is the porous parameter, α_1 and α_2 are the slip parameters. To find the electric force, $\rho_e E_x$, first we have to find the electric field E_x and then the charge density ρ_e using Maxwell's equations given by

Gauss's law,

$$\frac{\partial E_i}{\partial x_i} = \rho_e / \varepsilon_0 \tag{9}$$

Faraday's law, neglecting induced magnetic field because $\sigma \ll 1$, and there is no applied magnetic field,

$$\varepsilon_{ijk} \frac{\partial E_i}{\partial x_j} = 0 \Rightarrow E_i = -\frac{\partial \Phi}{\partial x_i} \tag{10}$$

Ampere's law,

$$\varepsilon_{ijk} \frac{\partial H_i}{\partial x_j} = J_i + \rho_e q_i \tag{11}$$

Solenoidal property of magnetic field

$$\frac{\partial H_i}{\partial x_i} = 0 \tag{12}$$

These equations have to be supplemented with the equation of continuity of charges

$$\frac{\partial \rho_e}{\partial t} + \frac{\partial (\rho_e q_i)}{\partial x_i} + \frac{\partial J_i}{\partial x_i} = 0 \tag{13}$$

and using ohms law for a poorly conducting media ($\sigma \ll 1$) and neglecting convection current $\rho_e q_i$ compared to conduction current and we denote $D_i = \varepsilon_0 E_i$, $J_i = \sigma E_i$. From these, while using the assumption $\sigma \ll 1$, Eq. (13) becomes

$$\frac{\partial \rho_e}{\partial t} + \sigma \frac{\partial E_i}{\partial x_i} + E_i \frac{\partial \sigma}{\partial x_i} = 0 \quad \left(\because \frac{\partial q_i}{\partial x_i} = 0 \right) \tag{14}$$

Further using Eqs. (9) and (10), and taking $\sigma = \sigma(\eta)$, we get

$$\frac{\partial^2 \Phi}{\partial \eta^2} + \frac{1}{\sigma} \frac{\partial \Phi}{\partial \eta} \frac{\partial \sigma}{\partial \eta} = 0 \tag{15}$$

with the boundary conditions due to potentials $\Phi = Vx/h$ at $y = 0$ and $\Phi = V(x - x_0)/h$ at $y = h$ due to embedded electrodes as shown in Fig. 1. Making Φ dimensionless using V, the boundary conditions are

$$\Phi = x - x_0 \quad \text{at} \quad \eta = 1; \qquad \Phi = x \quad \text{at} \quad \eta = 0 \tag{16}$$

Since $\sigma \ll 1$, perturbation on it is negligible and hence σ depends on the basic concentration C_b. Making σ dimensionless using σ_0, and using C_b the basic concentration obtained by solving $d^2 C_b / d\eta^2 = 0$ satisfying $C_b = C_0$ at $\eta = 0$ and $C = C_1$ at $\eta = 1$, in the form $C_b = (C_1 - C_0)\eta + C_0$. Then σ is given by

$$\sigma = 1 + \alpha \eta \approx e^{\alpha \eta} \quad (\text{since} \quad \alpha \ll 1) \tag{17}$$

where $\alpha = \alpha_h \triangle C, \triangle C = C_1 - C_0$. Eq. (15), using Eq. (17), becomes

$$\frac{d^2 \Phi}{d\eta^2} + \alpha \frac{d\Phi}{d\eta} = 0 \tag{18}$$

The solution of Eq. (18), using the boundary condition given in Eq. (16), is

$$\Phi = x - \frac{x_0(1 - e^{-\alpha\eta})}{1 - e^{-\alpha}} \tag{19}$$

Substituting Eq. (19) into E_x and ρ_e, we get

$$E_x = -\frac{\partial \Phi}{\partial x} = -1 \quad \text{and} \quad \rho_e = -\frac{\partial^2 \Phi}{\partial \eta^2} = \frac{x_0 \alpha^2 e^{-\alpha\eta}}{1 - e^{-\alpha}} \tag{20}$$

If C is the concentration of aerosols in the atmosphere, and diffuses in the atmospheric turbulent fluid of unidirectional flow given by Eqs. (2) and (3), then C, with first order chemical reaction, satisfies the equation

$$\frac{\partial C}{\partial t} + u^\beta \frac{\partial C}{\partial x} = D_e \left(\frac{\partial^2 C}{\partial x^2} + \frac{\partial^2 C}{\partial y^2} \right) - k_1 C \tag{21}$$

We study the electrohydrodynamic dispersion of aerosols by the atmospheric fluid and vice-versa using Taylor's model, in the next section.

3. Electrohydrodynamic dispersion of aerosols

The required basic equations and the corresponding boundary conditions are given by Eqs. (5) to (16). These equations are coupled linear partial differential equations (PDE). Although it is possible to decouple these equations using a suitable operator, the resulting PDE becomes higher order and cumbersome and the required boundary conditions have to be extrapolated. Therefore, we avoid this process and use a regular perturbation technique choosing $\varepsilon = R_2 R_3 \left(= K \mu_s t_0 / (\rho^s \mu_f) \right)$ to be small as a perturbation parameter. This assumption $K \mu_s / \rho^s \ll \mu_f / t_0$ is valid in our study of quasi-steady flow obtained following Taylor [1], where t_0 is very large and μ_f, the viscosity of atmospheric fluid, is small. In this technique, we look for solutions of Eqs. (5) and (6) in the form

$$u^f = u_0^f + \varepsilon u_1^f + ..., \qquad u^s = u_0^s + \varepsilon u_1^s + ... \tag{22}$$

Substituting Eqs. (22) and (20) into Eqs. (5) and (6) and assuming the normal mode solutions of the form

$$\{u_i^f(y,t), u_i^s(y,t), G(t)\} = \{u_i^f(y), u_i^s(y), G_0\}e^{-nt} \tag{23}$$

where $i = 0, 1, \ldots$, and on simplifying them, we get

$$\frac{d^2 u_0^s}{d\eta^2} - a_0^2 u_0^s = \phi^s - \frac{W_e}{R_1} e^{-\alpha\eta} \tag{24}$$

$$\frac{d^2 u_0^f}{d\eta^2} + b_0^2 u_0^f = \phi^f - \frac{\lambda R_2}{R_4} u_0^s - \frac{W_e}{R_4} e^{-\alpha\eta} \tag{25}$$

$$\frac{d^2 u_1^s}{d\eta^2} - a_0^2 u_1^s = -\frac{u_0^f}{R_1} \tag{26}$$

$$\frac{d^2 u_1^f}{d\eta^2} + b_0^2 u_1^f = \frac{\lambda}{R_4} u_0^f - \frac{\lambda R_2}{R_4} u_1^s \tag{27}$$

where $a_0^2 = (R_2 - n)/R_1$ and $b_0^2 = n/R_4$. The boundary conditions are the Saffman [14] slip conditions as given in Eq. (8), which become

$$\frac{du_i^s}{d\eta} = \pm \alpha_1 \sigma_p u_i^s, \quad \frac{du_i^f}{d\eta} = \pm \alpha_2 \sigma_p u_i^f \quad \text{at} \ \eta = 0, \ \text{and} \ 1 \ \text{for} \ t > 0, \text{respectively} \tag{28}$$

Similarly we can get equations for $i > 1$, but we restrict only to $i = 0$ and 1. The solutions of Eqs. (24) to (27), satisfying the condition given by Eq. (28), are

$$u_0^s = c_1 \cosh a_0 \eta + c_2 \sinh a_0 \eta - \frac{W_e e^{-\alpha\eta}}{R_1 \left(\alpha^2 - a_0^2\right)} - \frac{\phi^s}{a_0^2} \tag{29}$$

$$u_0^f = \Delta_{11} \cos b_0 \eta + \Delta_{12} \sin b_0 \eta + \Delta_{13} \cosh a_0 \eta + \Delta_{14} \sinh a_0 \eta + \Delta_{15} e^{-\alpha\eta} + \Delta_{16} \tag{30}$$

$$u_1^s = (\Delta_{17} + \Delta_{18}\eta)\sinh a_0 \eta + (\Delta_{19} + \Delta_{20}\eta)\cosh \eta + \Delta_{21}\sin b_0 \eta$$
$$+ \Delta_{22}\cos b_0 \eta + \Delta_{23}e^{-\alpha\eta} + \Delta_{24} \tag{31}$$

$$u_1^f = (\Delta_{25} + \Delta_{26}\eta)\cos b_0 \eta + (\Delta_{27} + \Delta_{28}\eta)\sin b_0 \eta + (\Delta_{29} + \Delta_{30}\eta)\cosh a_0 \eta$$
$$+ (\Delta_{31} + \Delta_{32}\eta)\sinh a_0 \eta + \Delta_{33}e^{-\alpha\eta} + \Delta_{34} \tag{32}$$

where the coefficients $\Delta_{1j}(j = 1, \ldots, 9)$, $\Delta_{2j}(j = 0, \ldots, 9)$, $\Delta_{3j}(j = 0, \ldots, 4)$, are given in the appendix of this paper.

From Eq. (22), using Eqs. (29) to (32), we get

$$u^s = u_0^s + \varepsilon u_1^s$$
$$= \left[(a_{11} + a_{12}\eta)\cosh a_0\eta + (a_{13} + a_{14}\eta)\sinh a_0\eta + a_{15}\sin b_0\eta \right. \tag{33}$$
$$\left. + a_{16}\cos b_0\eta + a_{17}e^{-\alpha\eta} + a_{18} \right]$$

$$u^f = u_0^f + \varepsilon u_1^f$$
$$= \left[(b_{11} + b_{12}\eta)\cos b_0\eta + (b_{13} + b_{14}\eta)\sin b_0\eta + (b_{15} + b_{16}\eta)\cosh a_0\eta \right. \tag{34}$$
$$\left. + (b_{17} + b_{18}\eta)\sinh a_0\eta + b_{19}e^{-\alpha\eta} + b_{20} \right]$$

where the coefficients a_{1i} $(i=1,...,8)$ and b_{1i} $(i=1,...,9)$, b_{20} are given in the appendix.

To find the concentration distribution, we assume, following Taylor [1], the longitudinal diffusion is much less than the transverse diffusion, which implies $\partial^2 C / \partial x^2 \ll \partial^2 C / \partial y^2$. Furthermore, we assume though there is a small longitudinal gradient of C along the flow, advection generates a small amount of aerosol across a section of the flow which moves with the mean speed. In other words, this small transport and the small longitudinal concentration gradient must be proportional to one another. Thus the combined effect of longitudinal advection and transverse diffusion is to disperse the aerosol longitudinally relative to a frame moving at the mean speed of flow by a mechanism which obeys the same law as an ordinary one-dimensional diffusion relative to fluid at rest. Then Eq. (19) takes the form

$$\frac{\partial C}{\partial t} + u^\beta \frac{\partial C}{\partial x} = D_e \frac{\partial^2 C}{\partial y^2} - k_1 C \tag{35}$$

In this paper, we consider two situations; one is for the advection of aerosols by the atmospheric fluid, and the other for the advection of atmospheric fluid by agglomeration, the solid phase of aerosol. These are discussed as follows.

3.1. Advection by atmospheric fluid

In this case, denoting $\beta = f$, Eq. (35) takes the form

$$\frac{\partial C}{\partial t} + u^f \frac{\partial C}{\partial x} = D_e \frac{\partial^2 C}{\partial y^2} - k_1 C \tag{36}$$

Making this equation dimensionless using the scales

$$C^* = \frac{C}{C_0}, \quad t^* = \frac{t}{t_0}, \quad \eta = \frac{y}{h}, \quad \text{and} \quad \xi = \frac{x - \bar{u}^f t}{L}, \quad u^{f*} = \frac{u^f}{U} \tag{37}$$

where c_0 is the initial slug, L is the characteristic length along this flow direction, $U = h^2 G_0 / \mu_f$ is the characteristic velocity and all other scales are the same as defined in Eq. (4) and

$$\bar{u}^f = \int_0^1 u^f \, d\eta = F \tag{38}$$

is the average fluid velocity, where

$$F = \left(\frac{b_{11} + b_{12}}{a_0} - \frac{b_{14}}{a_0^2} \right) \sinh a_0 - \left(\frac{b_{13} + b_{14}}{a_0} - \frac{b_{12}}{a_0^2} \right) \cosh a_0 + \left(\frac{b_{15} + b_{16}}{b_0} - \frac{b_{18}}{b_0^2} \right) \sin b_0$$
$$- \left(\frac{b_{17} + b_{18}}{b_0} - \frac{b_{16}}{b_0^2} \right) \cos b_0 + \left(\frac{b_{12}}{a_0^2} - \frac{b_{13}}{a_0} + \frac{b_{16}}{b_0^2} + \frac{b_{17}}{a_0} \right) + b_{19} \tag{39}$$

and for simplicity neglecting the asterisks, we get

$$\frac{1}{t_0} \frac{\partial C}{\partial t} + \frac{w^f}{L} \frac{\partial C}{\partial \xi} = \frac{D}{h^2} \frac{\partial^2 C}{\partial \eta^2} - k_1 C \tag{40}$$

where

$$w^f = u^f - \bar{u}^f = (b_{11} + b_{12}\eta) \cosh a_0 \eta + (b_{13} + b_{14}\eta) \sinh a_0 \eta + (b_{15} + b_{16}\eta) \cos b_0 \eta$$
$$+ (b_{17} + b_{18}\eta) \sin b_0 \eta - f_0, \tag{41}$$

where $f_0 = F - b_{19}$, and $b_{1i} (i = 1, \ldots, 9)$ are constants given in the appendix.

Following Taylor [1], we assume the partial equilibrium at any cross-section of the layer and obtain concentration as a function of y by approximating Eq. (36) in the form

$$\frac{\partial^2 C}{\partial \eta^2} - \beta_1^2 C = D_1 w^f \tag{42}$$

where $D_1 = (h^2 / DL)(\partial C / \partial \xi)$ and $\beta_1^2 = h^2 k / D_e$ is the reaction rate parameter. For compatibility with the atmospheric layer we solve this equation for permeable to concentration given by

$$C = 1 \quad \text{at} \quad \eta = 0, \quad \frac{\partial C}{\partial \eta} = 0 \quad \text{at} \quad \eta = 1 \tag{43}$$

The solution of Eq. (42), after using Eqs. (41) and (43), we get

$$C = c_1 \cosh \beta_1 \eta + c_2 \sinh \beta_1 \eta + D_1)(e_{11} + e_{12}\eta)\cosh a_0 \eta + (e_{13} + e_{14}\eta)\sinh a_0 \eta$$
$$- (e_{15} + e_{16}\eta)\cos b_0 \eta - (e_{17} + e_{18}\eta)\sin b_0 \eta + \frac{f_0}{\beta_1^2} \tag{44}$$

where c_1, c_2 and $e_{1i}, (i = 1, ..., 7)$ are constants and are given in the appendix. The volumetric rate at which the aerosol is transported across a section of a layer of unit breadth is

$$M = \int_0^1 C w^f \, d\eta \tag{45}$$

Hence, using Eqs. (44) and (45), performing the integration and after simplification, we get

$$M = \frac{N_1^f h^2}{L D_e} \frac{\partial C}{\partial \xi} + 1 \tag{46}$$

where $N_1^f = \int_0^1 D_1^{-1}(C - 1) w^f \, d\eta$. Following Taylor [1], we assume that the variation of C with y is small compared to the longitudinal direction and if C_m is the mean concentration over a section, then $\partial C / \partial \xi$ is indistinguishable from $\partial C_m / \partial \xi$ so that Eq. (46) can be written as

$$M = \frac{N_1^f h^2}{L D_e} \frac{\partial C_m}{\partial \xi} + 1 \tag{47}$$

This shows that C_m will be dispersed relative to plane which moves with the mean velocity $\bar{u}^f$ exactly as though it is being diffused by a process which obeys the same law as molecular diffusion but with a relative diffusion coefficient

$$D^f = -N_1^f \frac{h \bar{u}^f}{D_e} = N^f P e^f \tag{48}$$

called Taylor diffusion coefficient for the mixture of deformable agglomeration and atmospheric fluid, $Pe^f = h\bar{u}^f / D_1$ is the Peclet number and

$$N^f = -N_1^f = -\int_0^1 \left(\frac{C-1}{D_1} \right) w^f d\eta. \tag{49}$$

and w^f is given in Eq. (41) This is integrated using Eqs. (44) and (41). The fact that no material is lost in the process is expressed by the continuity equation for C_m namely

$$\frac{\partial M}{\partial \xi} = -\frac{1}{L} \frac{\partial C_m}{\partial t} \tag{50}$$

where the time derivative pertains to a point at which ξ is fixed. Eq. (47), using Eqs. (49) and (50), takes the form

$$\frac{\partial C_m}{\partial t} = D^f \frac{\partial^2 C_m}{\partial \xi^2} \tag{51}$$

This equation represents the longitudinal dispersion of deformable agglomeration in the atmospheric fluid and dispersed with the dispersion coefficient D^f given by Eq. (48). This is computed for different values of electric number W_e , Reynolds number Re , Peclet number Pe and reaction rate parameter β_1, and the results are depicted graphically and are discussed in section 4.

3.2. Advection by agglomeration of aerosol

We also note that the advection of atmospheric fluid by agglomeration can also be discussed following the analysis of section 3.1 by substituting $\beta = s$ in Eq. (35). Following the same procedure as explained in section 3.1, we get

$$D^s = Pe^s N^s \tag{52}$$

where $Pe^s = h\bar{u}^s / D_m$ and

$$N^s = -\int_0^1 \left(\frac{C-1}{D_1} \right) w^s d\eta \tag{53}$$

As in Eq. (49), this is integrated using w^s and $C-1$ and the D^s is computed for different values of electric number W_e, Reynolds number Re , Peclet number Pe and the reaction rate parameter β_1, the results are depicted graphically and are

discussed in the next section.

4. Results and Discussions

One of the necessary tasks associated with industrialization is to achieve progress in the removal of solid or liquid particles from gases discharged to the environment. Design of optimized pollution control devices becomes increasingly important towards achieving that goal. Fibrous filters are effective in the removal of submicrometer aerosol particles but their application is limited to low concentrations of aerosol dust in air. On the other hand, cyclones are efficient only at high gas flow rates and for larger particles. Cyclones, although very common devices, are still objects of intensive research because of their wide range of applications. In the case of smaller aerosol particulates an increase in the collection efficiency of particles in the turbulent flow is necessary. An application of an externally applied electric field in a turbulent flow assisting the inertial removal effect should result in increased cleaning effectiveness, in particular for small particles of poorly conducting materials. A standard design cyclone, with a tangential inlet in which an electric field is generated in the space between an external wall and the central outlet channel is considered. The dispersion of large size deformable aerosols mixed with a poorly conducting atmospheric fluid is discussed in this paper analytically using Taylor's model valid asymptotically for large time with the objective of understanding the effect of electric field on the dispersion of atmospheric aerosols because of its importance in the applications mentioned above. The dispersion of deformable agglomeration in quasi-steady flow is discussed in Section 3. The equations governing the flow for atmospheric fluid, poorly conducting fluid and for deformable agglomeration obtained under the assumption of fully developed flow are the coupled partial differential Eqs. (5) and (6). These equations are solved analytically using regular perturbation technique given by Eq. (22) with $\varepsilon = K \mu_s t_0 / (\rho^s \mu_f) \ll 1$. This assumption is valid in our study of quasi-steady flow as considered in Rudraiah and Ng [16]. Using these approximations and following the analysis of Taylor we obtained the solutions analytically. Using these solutions the dispersion coefficient D^β is determined as given by Eq. (48) for advection by atmospheric fluid $(\beta = f)$ and by Eq. (52) for advection by agglomeration $(\beta = s)$. The results are represented graphically. Figures 2 and 3 represent the effect of electric number on the velocity

profiles of atmospheric fluid and aerosols. From these figures we find that u^f increases with We, because electric field induces a small scale turbulence but decreases with an increase in σ_p because the permeability dampens the velocity profile. Figure 4 represents the effect of porous parameter on the dispersion of aerosols in a atmospheric poorly conducting fluid for different values of Reynolds number Re and it shows that the dispersion coefficient D^f decreases with an increase in porous parameter because of its dampening effect but increases with an increase in Reynolds number. Figures 5 and 7 show the effect of deformation parameter on the dispersion coefficient D^s for different values of Reynolds number and this figure shows that the D^s decreases for small values of R_1 up to 0.2 and for higher values from 0.25 it remains uniform. It also reveals that increase in Re slightly increases for values R_1 up to 0.5 and for $R_1 > 0.5$, D^f remains uniform. Figure 6 shows that D^f decreases with an increase in R_1 up to 0.5 and also decreases with an increase in Pe up to $R_1 = 0.5$ and then remain uniform with respect to increase in R_1 and Pe. Figure 7 shows that D^s decreases with an increase in R_1 and for $R_1 > 0.7$ it tends to unity. However, D^s decreases with an increase in Pe up to 100 and tends to 10^{21} at $R_1 = 1$ and for $Pe > 100$ it increases. Figure 8 shows that the D^f increases with an increase in We for $Pe = 150$. Similarly, Figure 9 shows that D^f increases with an increase in reaction rate parameter β_1 for $We = 50$ and $Re = 10^3$ and reaches the maximum value 4.5×10^{24} for $\beta_1 = 40$.

5. Conclusions

In this paper we investigated the effect of electric field and the first order chemical reaction on the dispersion of aerosols in a channel bounded by porous layers using Taylor's model. Analytical solutions for velocities and concentration distributions are obtained using a regular perturbation technique. It is shown that the aerosols are dispersed relative to a plane moving with the mean speed of atmospheric fluid as well as the mean speed of agglomeration of aerosol with a relative diffusion coefficient, called Taylor dispersion coefficient. This dispersion coefficient is numerically computed and the results reveal that the electric field and chemical reaction enhances

the transport (dispersion) of aerosols, i.e., the electric field removes efficiently the solid or liquid particles from gases discharged to the environment. Therefore, results through a light on aerosol removal mechanisms. Also, it is found that the transport of aerosols decreases with an increase in the porous parameter.

Appendix

$$\Delta = \left(a_0^2 + \alpha_1^2 \sigma^2 \right) \sinh a_0 + 2 a_0 \alpha_1 \sigma \cosh a_0,$$

$$\delta = a_0 \sinh a_0 + \alpha_1 \sigma \cosh a_0,$$

$$c_1 = \frac{W_e(\alpha - \alpha_1 \sigma)}{\alpha_1 \sigma R_1(\alpha^2 - a_0^2)} + \frac{\varphi^s}{a_0^2}$$
$$+ \frac{a_0}{\Delta \alpha_1 \sigma} \left(\frac{W_e(\alpha_1 \sigma - \alpha)\delta}{R_1(\alpha^2 - a_0^2)} - \frac{\alpha_1 \sigma \delta \varphi^s}{a_0^2} + \frac{W_e e^{-\alpha} \alpha_1 \sigma(\alpha_1 \sigma - \alpha)}{R_1(\alpha^2 - a_0^2)} + \frac{\alpha_1^2 \sigma^2 \varphi^s}{a_0^2} \right),$$

$$c_2 = \frac{1}{\Delta} \left(\frac{W_e(\alpha_1 \sigma - \alpha)\delta}{R_1(\alpha^2 - a_0^2)} - \frac{\alpha_1 \sigma \delta \varphi^s}{a_0^2} + \frac{W_e e^{-\alpha} \alpha_1 \sigma(\alpha_1 \sigma - \alpha)}{R_1(\alpha^2 - a_0^2)} + \frac{\alpha_1^2 \sigma^2 \varphi^s}{a_0^2} \right),$$

$$c_3 = l_2 + \frac{b_0(l_1 - l_2)(\alpha_2 \sigma \cos b_0 - b_0 \sin b_0)}{(\alpha_2^2 \sigma^2 - b_0^2)\sin b_0 + 2 b_0 \alpha_2 \sigma \cos b_0}, \qquad c_4 = \frac{(c_3 - l_3)\alpha_2 \sigma}{b_0},$$

$$l_1 = \frac{\lambda R_2 c_1 a_0 \sinh a_0}{R_4(a_0^2 + b_0^2)} + \frac{\lambda R_2 c_2 a_0 \cosh a_0}{R_4(a_0^2 + b_0^2)} + \frac{\alpha e^{-\alpha} W_e}{(\alpha^2 + b_0^2)} \left(\frac{\lambda R_2}{R_1 R_4(\alpha^2 - a_0^2)} - \frac{1}{R_4} \right) - \frac{\alpha_2 \sigma \varphi^f}{b_0^2}$$
$$+ \frac{\alpha_2 \sigma \lambda R_2 c_1 \cosh a_0}{R_4(a_0^2 + b_0^2)} + \frac{\alpha_2 \sigma \lambda R_2 c_2 \sinh a_0}{R_4(a_0^2 + b_0^2)} - \frac{\alpha \sigma e^{-\alpha} W_e}{(\alpha^2 + b_0^2)} \left(\frac{\lambda R_2}{R_1 R_4(\alpha^2 - a_0^2)} - \frac{1}{R_4} \right) - \frac{\alpha_2 \sigma \lambda R_2 \varphi^s}{R_4(a_0^2 + b_0^2)},$$

$$l_2 = \frac{-\lambda R_2 c_2 a_0}{\alpha_2 \sigma R_4(a_0^2 + b_0^2)} - \frac{\alpha W_e}{\alpha_2 \sigma(a_0^2 + b_0^2)} \left(\frac{\lambda R_2}{R_1 R_4(\alpha^2 - a_0^2)} - \frac{1}{R_4} \right) - \frac{\varphi^f}{b_0^2}$$
$$+ \frac{\lambda R_2 \sigma c_1}{R_4(a_0^2 + b_0^2)} - \frac{W_e}{\alpha^2 + b_0^2} \left(\frac{\lambda R_2}{R_1 R_4(\alpha^2 - a_0^2)} - \frac{1}{R_4} \right) - \frac{\lambda R_2 \varphi^s}{R_4(a_0^2 b_0^2)},$$

$$l_3 = \left(c_4 b_0 + \frac{\lambda R_2 c_2}{2 a_0 R_4} \right) \frac{1}{\alpha_1 \sigma R_1(a_0^2 + b_0^2)} - \frac{\alpha W_e(\lambda R_2 + R_1)}{\alpha_1 \sigma R_1 R_4(\alpha^2 - a_0^2)(\alpha^2 + b_0^2)} - \frac{c_3}{R_1(a_0^2 + b_0^2)}$$
$$- \frac{(\lambda R_2 + R_1)W_e}{R_1 R_4(\alpha^2 - a_0^2)^2(\alpha^2 + b_0^2)} + \frac{\lambda R_2 \varphi^s}{R_4 a_0^4 b_0^2},$$

$$l_4 = \frac{1}{\Delta} \left[\frac{b_0(c_3 \sin b_0 - c_4 \cos b_0)}{R_1(a_0^2 + b_0^2)} - \frac{\lambda R_2[(c_1 a_0 + c_2)\cosh a_0 + (c_1 + c_2 a_0)\sinh a_0]}{2 a_0 R_1 R_4(a_0^2 + b_0^2)} \right.$$
$$+ \frac{W_e \alpha e^{-\alpha}(\lambda R_2 - R_1)}{R_1 R_4(\alpha^2 - a_0^2)(a_0^2 - b_0^2)} \frac{\alpha_1 \sigma(c_3 \cos b_0 + c_4 \sin b_0)}{R_1(a_0^2 + b_0^2)} - \frac{\alpha_1 \sigma \lambda R_2(c_1 \sinh a_0 + c_2 \cosh a_0)}{2 a_0 R_1 R_4(a_0^2 + b_0^2)}$$
$$\left. - \frac{W_e \alpha_1 \sigma e^{-\alpha}(\lambda R_2 - R_1(\alpha^2 - a_0^2))}{R_1 R_4(\alpha^2 - a_0^2)^2(\alpha^2 + b_0^2)} \right],$$

$$\Delta_{11} = l_2 + \frac{b_0(l_1 - l_2)(\alpha_2\sigma\cos b_0 - b_0\sin b_0)}{(\alpha_2^2\sigma^2 - b_0^2)\sin b_0 + 2b_0\alpha_2\sigma\cos b_0}, \quad \Delta_{12} = \frac{b_0(l_1 - l_2)(\alpha_2\sigma\cos b_0 - b_0\sin b_0)}{(\alpha_2^2\sigma^2 - b_0^2)\sin b_0 + 2b_0\alpha_2\sigma\cos b_0},$$

$$\Delta_{13} = \frac{-\lambda R_2 c_1}{R_4(a_0^2 + b_0^2)}, \quad \Delta_{14} = \frac{-\lambda R_2 c_2}{R_4(a_0^2 + b_0^2)}, \quad \Delta_{15} = \left(\frac{-\lambda R_2}{R_1 R_4(\alpha^2 + b_0^2)} - \frac{1}{R_4}\right)\frac{W_e}{\alpha^2 + b_0^2},$$

$$\Delta_{16} = \frac{\lambda R_2 \varphi^s}{R_4 a_0^2 b_0^2} + \frac{\varphi^f}{b_0^2}, \quad \Delta_{17} = \frac{(l_4 - l_3)\alpha_2\sigma(a_0\sinh a_0 + \alpha_1\sigma\cosh a_0)}{(a_0^2 + \alpha_1^2\sigma^2)\sinh a_0 + 2a_0\alpha_1\sigma\cosh a_0},$$

$$\Delta_{18} = \frac{\lambda R_2 c_1}{2a_0 R_1 R_4(a_0^2 + b_0^2)}, \quad \Delta_{19} = l_3 + \frac{a_0}{\alpha_1\sigma}\Delta_{17}, \quad \Delta_{20} = \frac{\lambda R_2 c_2}{2a_0 R_1 R_4(a_0^2 + b_0^2)},$$

$$\Delta_{21} = \frac{c_4}{R_1(a_0^2 + b_0^2)}, \quad \Delta_{22} = \frac{c_3}{R_1(a_0^2 + b_0^2)},$$

$$\Delta_{23} = \left(\frac{\lambda R_2}{R_1 R_4(\alpha^2 - a_0^2)^2} - \frac{1}{R_4(\alpha^2 - a_0^2)}\right)\frac{W_e}{\alpha^2 + b_0^2}, \quad \Delta_{24} = -\left(\frac{\lambda R_2 \varphi^s}{R_4 a_0^4 b_0^2} + \frac{\varphi^f}{a_0^2 b_0^2}\right),$$

$$\Delta_{25} = l_6 - \frac{\alpha_2\sigma\delta(l_6 - l_5)}{\alpha_2\sigma\delta + b_0}, \quad \Delta_{26} = -\frac{\lambda_2}{2b_0}, \quad \Delta_{27} = \frac{\alpha_2\sigma(l_6 - l_5)}{\alpha_2\sigma\delta + b_0}, \quad \Delta_{28} = \frac{\lambda_1}{2b_0},$$

$$\Delta_{29} = -\left(\frac{\lambda_3}{a_0^2 + b_0^2} - \frac{2a_0\lambda_6}{(a_0^2 + b_0^2)}\right), \quad \Delta_{30} = -\left(\frac{\lambda_5}{a_0^2 + b_0^2}\right),$$

$$\Delta_{31} = -\left(\frac{\lambda_4}{a_0^2 + b_0^2} - \frac{2a_0\lambda_5}{(a_0^2 + b_0^2)^2}\right), \quad \Delta_{32} = -\frac{\lambda_6}{a_0^2 + b_0^2},$$

$$\Delta_{33} = -\frac{\lambda_7}{\alpha^2 + b_0^2}, \quad \Delta_{34} = -\frac{\lambda_8}{b_0^2},$$

$$a_{11} = c_1 + \varepsilon\Delta_{19}, \quad a_{12} = \varepsilon\Delta_{26}, \quad a_{13} = c_2 + \varepsilon\Delta_{17}, \quad a_{14} = \varepsilon\Delta_{18}, \quad a_{15} = \varepsilon\Delta_{21},$$

$$a_{16} = \varepsilon\Delta_{22}, \quad a_{17} = \frac{-W_e}{R_1(\alpha^2 - a_0^2)} + \varepsilon\Delta_{23}, \quad a_{18} = \frac{-\varphi^s}{a_0^2} + \varepsilon\Delta_{24}, \quad b_{11} = \Delta_{11} + \varepsilon\Delta_{25},$$

$$b_{12} = \varepsilon\Delta_{26}, \quad b_{13} = \Delta_{12} + \varepsilon\Delta_{27}, \quad b_{14} = \varepsilon\Delta_{28}, \quad b_{15} = \Delta_{13} + \varepsilon\Delta_{29}, \quad b_{16} = \varepsilon\Delta_{30},$$

$$b_{17} = \Delta_{14} + \varepsilon\Delta_{31}, \quad b_{18} = \varepsilon\Delta_{32}, \quad b_{19} = \Delta_{15} + \varepsilon\Delta_{33}, \quad b_{20} = \Delta_{16} + \varepsilon\Delta_{34}$$

References

[1]   TAYLOR G. I. Dispersion of soluble matter in solvent flowing slowly through a tube[J]. **Proc. Roy. Soc Lond. A**, 1953, 219(1137): 186-203.

[2]   WATERMAN P. C. Matrix formulation of scattering[J]. **Proc. IEEE,** 1965, 53**:** 805-812.

[3]   WILLIAMS T. J. and BAILEY A. G. Changes in the size distribution of a water-in-oil emulsion due to electric-field induced coalescence[J]. **IEEE Trans. Ind. Appl.,** 1986, 22(3)**:** 536-541.

[4]   SCHMIDT J. J. Experimental study of electro-coalescence in a unit reactor[D]. Master Thesis, University of Texas, 2000.

[5]   SUN LEI, LIN JIANZHONG, BAO FUBING Numerical simulation on the deposition of nanoparticles under laminar conditions[J]. **J. Hydrodynamics,** 2006,18(6): 676-680.

[6]   GAN FUJUN, LIN JIANZHONG, YU MINGZHOU Particle size distribution in a planar jet flow undergoing shear-induced coagulation and breakage[J]. **J. Hydrodynamics,** 2010, 22(4): 445-455.

[7]   YIN ZHAOQIN and LIN JIANZHONG Numerical simulation of the formation of nano-particles in an impinging twin-jet[J], **J. Hydrodynamics**, 2007, 19(6): 533-541.

[8]   LIU SONG and LIN JIANZHONG, Numerical simulation of nanoparticle coagulation in a Poiseuille flow via a moment method[J]. **J. Hydrodynamics**, 2008, 20(1): 1-9.

[9]   WANG H., ZENG S., LOEWENBERG M. and DAVIS R. H. Particle aggregation due to combined gravitational and electrophoretic motion[J]. **J. Colloid Interface Sci.,** 1997, 187(1)**:** 213-220.

[10]   JAYARATNE E. R. and VERMA T. S. Environmental aerosols and their effect on the Earth's local fair-weather electric field[J]. **Meteorol. Atmos. Phys.,** 2004, 86(3-4): 275-280.

[11]   RUDRAIAH N. and DEVARAJU N. Effects of the reaction rate and the large size deformable aerosols on dispersion in atmospheric flow regarded as the turbulent fluid saturated porous media[J]. **J. Porous Media**, 2011 (in press).

[12]   KENYON D. E. A Mathematical model of water flux through aortic tissue[J]. **Bull. Math. Bio.,** 1979, 41(1): 79-90.

[13]   BOWEN R. M. Incompressible porous-media models by use of the theory of mixtures[J]. **Int. J. Engg. Sci.,** 1980, 18(9): 1129-1148.

[14]   BARRY S. I., PARKER K. H. and ALDIS G. K. Fluid flow over a thin deformable porous layer[J]. **J. Appl. Math. Phys. (ZAMP),** 1991, 42(5): 633-648.

[15]   SAFFMAN P. G. On the boundary condition at surface of a porous medium[J]. **Stud. Appl. Math.,** 1971, 50(2): 93-101.

[16]   RUDRAIAH N. and NG C. O. Dispersion in porous media with and without reaction: a review[J]. **J. Porous Media**, 2007, 10(3), 219-248.
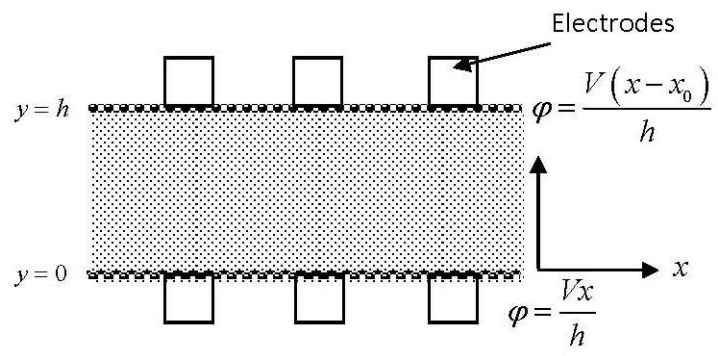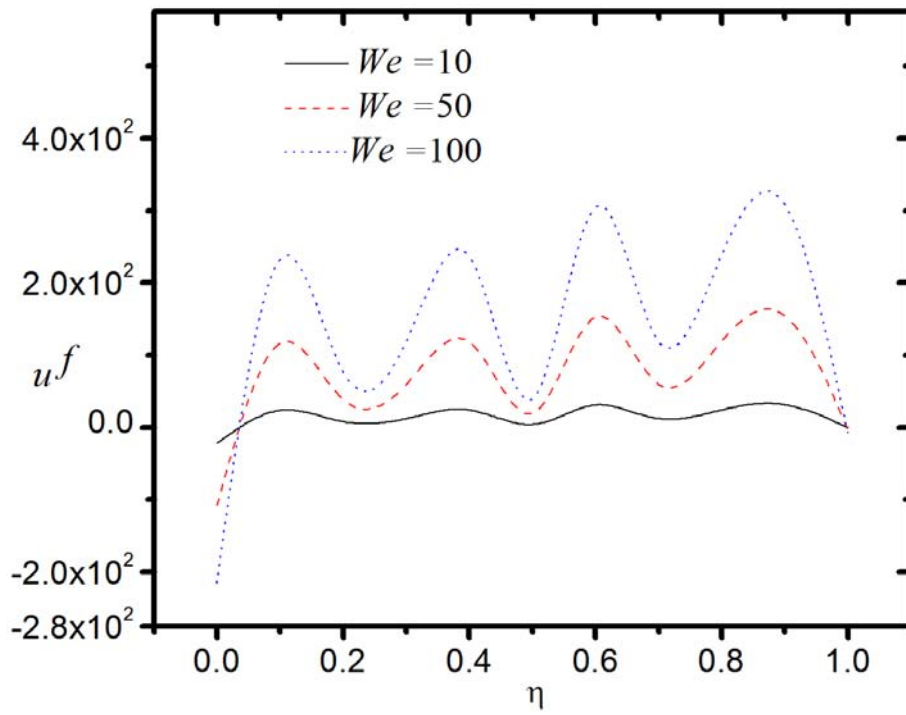
Figure Captions

FIGURE 1: Physical configuration.

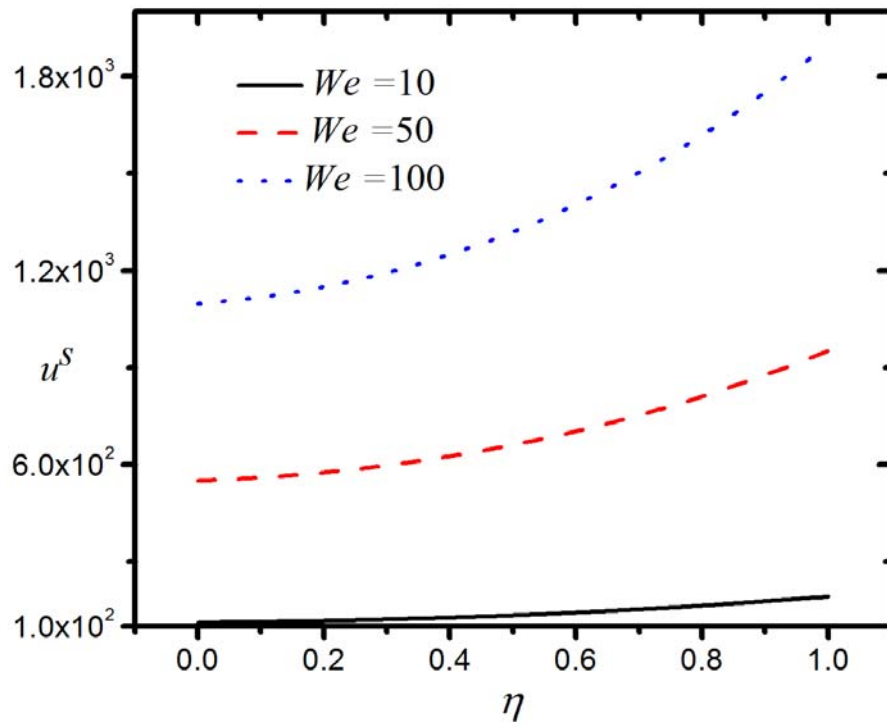FIGURE 2: Velocity profile for atmospheric fluid for different values of electric number We.

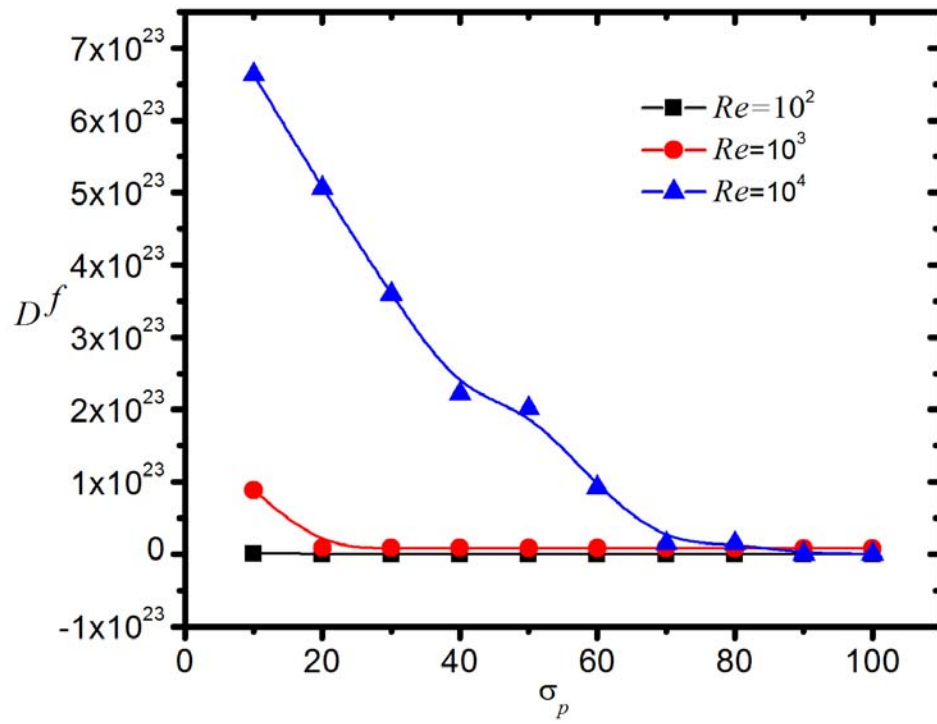FIGURE 3: Velocity profile of aerosols for different values of electric number We.

FIGURE 4: Dispersion coefficient D^f versus porous parameter for different Re.

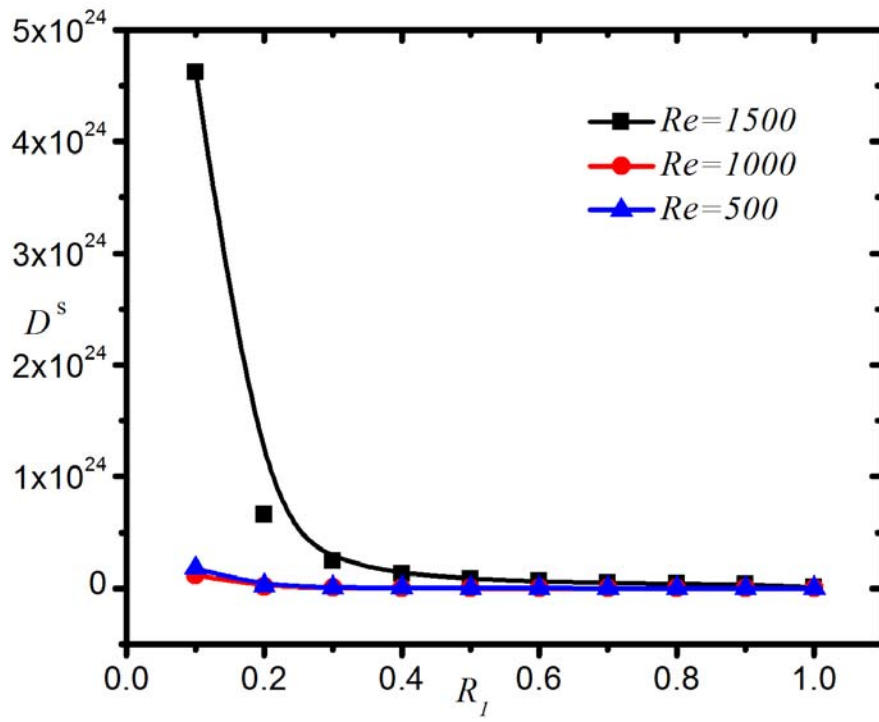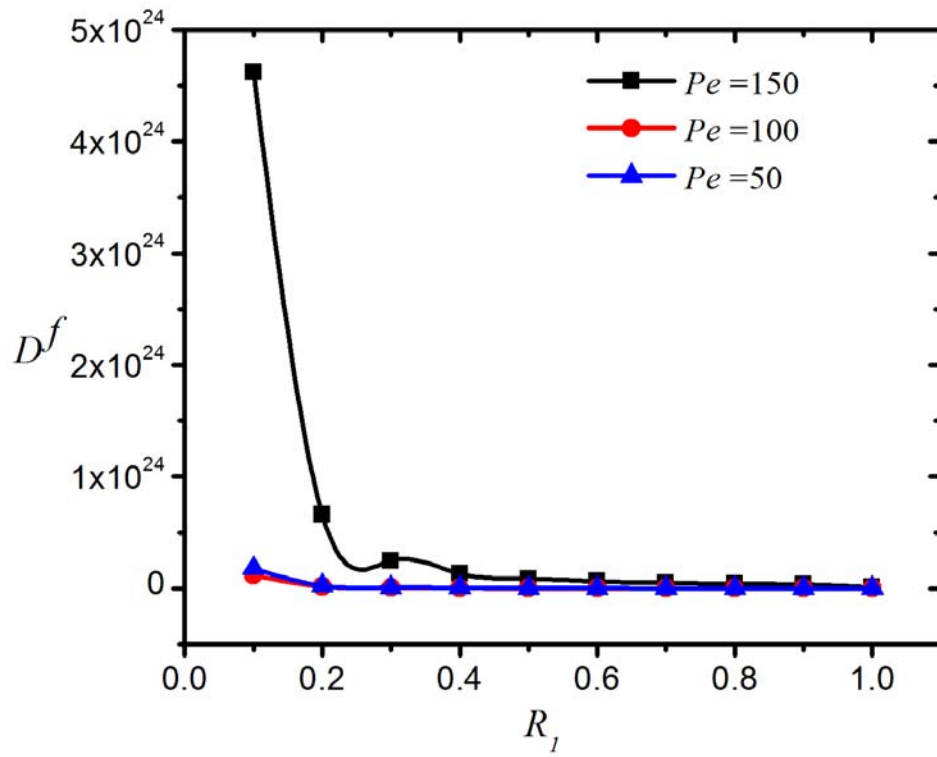FIGURE 5: Dispersion coefficient D^s versus deformation parameter for different Re.

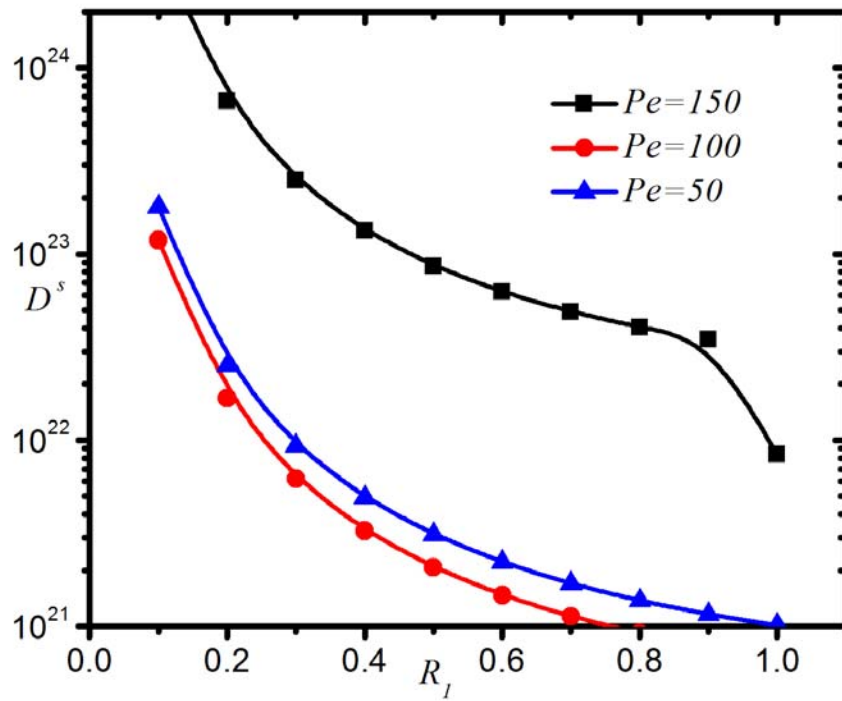FIGURE 6: Dispersion coefficient D^f versus deformation parameter for different Pe.

FIGURE 7: Dispersion coefficient D^s versus deformation parameter for different Pe.

FIGURE 8: Dispersion coefficient D^f versus electric number.

FIGURE 9: Dispersion coefficient D^f versus reaction rate parameter.

FIGURE 1: Physical configuration.

FIGURE 2: Velocity profile for atmospheric fluid for different values of electric number We.

FIGURE 3: Velocity profile of aerosols for different values of electric number *We*.

FIGURE 4: Dispersion coefficient D^f versus porous parameter for different Re.

FIGURE 5: Dispersion coefficient D^s versus deformation parameter for different Re.

FIGURE 6: Dispersion coefficient D^f versus deformation parameter for different Pe.

FIGURE 7: Dispersion coefficient D^s versus deformation parameter for different Pe.
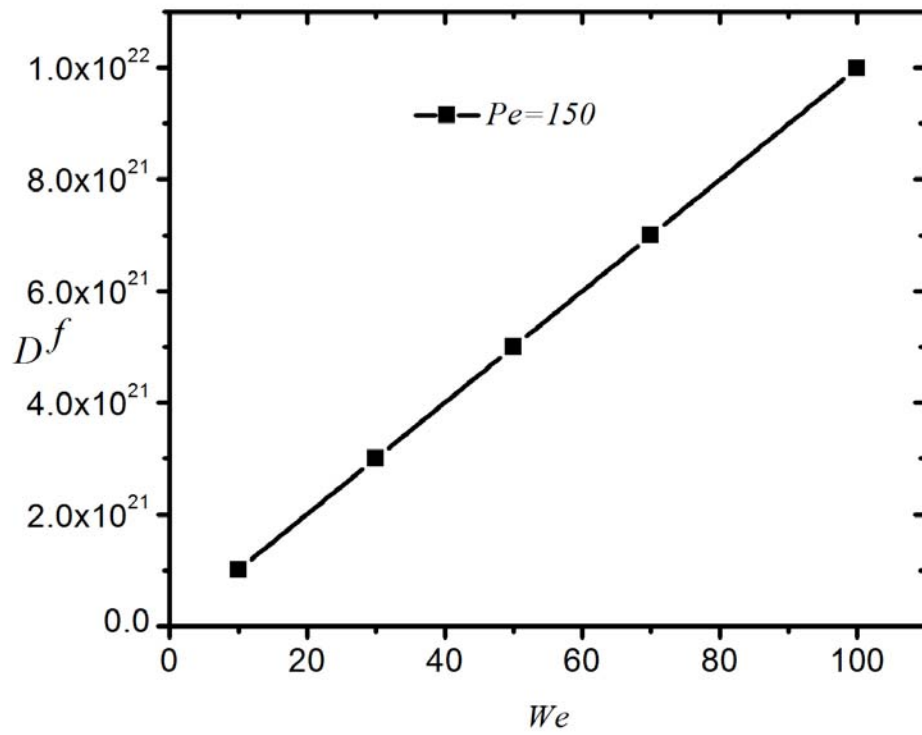
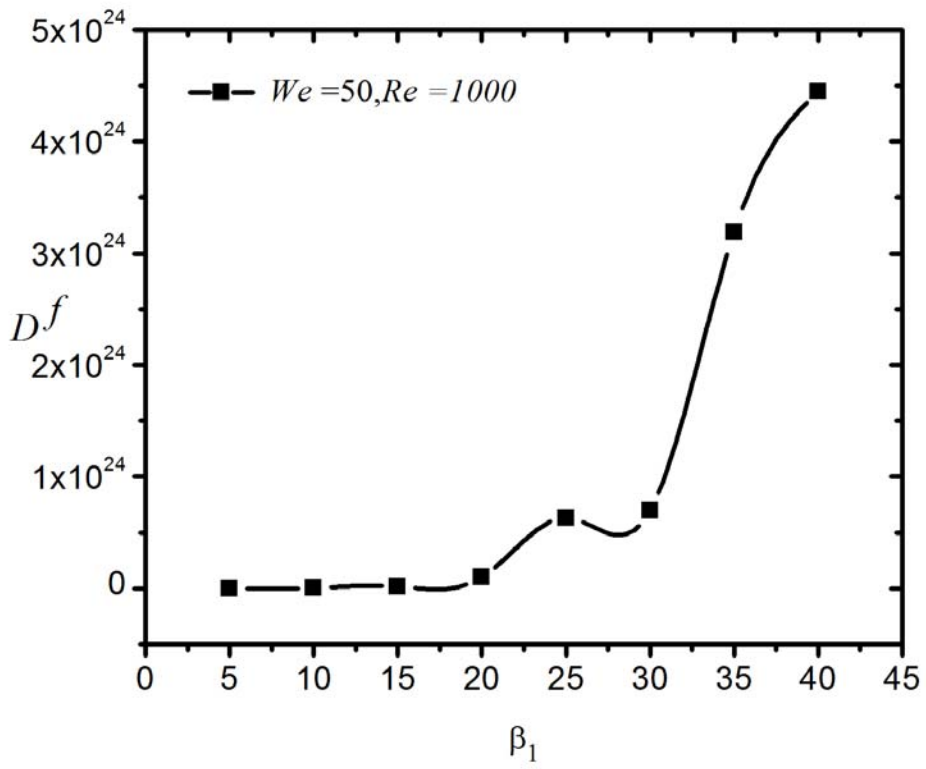FIGURE 8: Dispersion coefficient D^f versus electric number.

FIGURE 9: Dispersion coefficient D^f versus reaction rate parameter.